ELSEVIER

Journal of Organometallic Chemistry 550 (1998) 131–139

Journal of Organometallic Chemistry

Metal core rearrangements in hetero-bimetallic nona-osmium carbonyl clusters; the crystal and molecular structures of $[Os_9(CO)_{24}\{Au(PCy_3)\}_2]$ and $[Os_9(CO)_{23}(Au_2DPPE)]$ [1]

Zareen Akhter, Scott L. Ingham, Jack Lewis, Paul R. Raithby *

Department of Chemistry, Lensfield Road, Cambridge CB2 1EW, UK

Received 29 January 1997

Abstract

The reaction of the nona-osmium cluster dianion $[(Ph_3P)_2N]_2[Os_9(CO)_{24}]$ with the electrophilic gold reagents ''$AuPR_3^+$'' and ''Au_2L^{2+}'' (where R = Ph (**2a**, **3a**), Cy (**2b**, **3b**) and L = bis-(diphenylphosphino)methane (DPPM) (**1a**) or 1,2-bis-(diphenyl)ethane (DPPE) (**1b**)) has been studied. The monogold fragment reacts to give both the mono- and di-substituted products $[(Ph_3P)_2N][Os_9(CO)_{24}\{Au(PR_3)\}]$ and $[Os_9(CO)_{24}\{Au(PR_3)\}_2]$. The structure of the latter cluster (R = Cy (**2b**)) has been determined by a single crystal X-ray diffraction analysis and a major rearrangement of the metal core geometry was found to have occurred on coordination of the gold fragments. In contrast, reaction with the digold reagent ''Au_2L^{2+}'' results in the isolation of only one product of formulation $[Os_9(CO)_{23}(Au_2L)]$, where coordination of the heteroatom moiety has been accompanied with the loss of a carbonyl ligand. From a single crystal X-ray diffraction analysis (L = DPPE (**1b**)) this compound was shown to have retained its original cluster geometry, with the gold atoms coordinated in close proximity to each other. © 1998 Elsevier Science S.A.

Keywords: Osmium; Gold; Cluster carbonyls; X-ray structure; Phosphines

1. Introduction

There has been considerable interest in synthesis of hetero-bimetallic compounds because of the polarity that the heterometallic bond introduces to the molecule. This polarity difference may enhance any electrochemical or photochemical reactivity that the molecule possesses [1] and, as such, hetero-bimetallic compounds are of interest due to their possible applications in materials science. Large polynuclear metal-carbonyl clusters also exhibit unusual physicochemical properties due to the relationship between electronic delocalisation and the number of metal atoms within the cluster. Therefore, it is not surprising that in recent years there has been an increasing collection of compounds synthesised which are comprised of a large polynuclear metal-carbonyl cluster and incorporate some degree of hetero-bimetallic bonding [2]. The synthesis of many of these compounds has been achieved by the use of redox condensation reactions between anionic carbonyl compounds and neutral or cationic metal electrophiles, with the use of mercury and gold fragments being particularly successful [3].

The number of high nuclearity metal-carbonyl clusters that have been structurally characterised has steadily increased in recent years. It has been observed that many of these compounds no longer obey the classical electron counting rules which have been so widely employed to rationalise the structures of their lower nuclearity counterparts [4]. This apparent breakdown in the electron counting rules reflects the delocalised electronic nature within the metal framework. As such, the metal–metal interaction within these species may be thought to lie at the interface between the localised bonding involved in classical organometallic compounds and the high electron mobility that is an intrinsic property of metallic solids. A consequence of the increasing electron delocalisation within high nuclearity metal-carbonyl clusters is that the metal–metal bonding

* Corresponding author.

[1] Dedicated to Professor Ken Wade on the occasion of his 65th birthday in recognition of his outstanding contributions to organometallic and inorganic chemistry.

may be thought to consist of a significant proportion of s-character and, as such, has considerably more directional flexibility. As a result of this increased flexibility within the metal core, the introduction of a heterometallic fragment may perturb the cluster framework, either as a consequence of the formation of the new polar metal–metal bond, or arising from the steric constraints of the incoming group.

We have recently shown [5] that the reaction between the anionic cluster $[(Ph_3P)_2N]_2[Os_8(CO)_{22}]$ and gold electrophilic fragments results in a subtle balance between the kinetically and thermodynamically favoured products. It was noted that the thermodynamic product resulted in a significant metal core rearrangement and that this transformation proceeded smoothly at ambient temperatures. However, it was observed that the kinetic product could be stabilised and isolated by the use of a digold fragment linked with a bidentate phosphine. In an attempt to further explore this unusual reactivity and to investigate what effect increasing cluster size may have upon it, we now report the results of a study of the interactions between the high nuclearity cluster dianion $[(Ph_3P)_2N]_2[Os_9(CO)_{24}]$ [6] and selected electrophilic gold reagents.

2. Results and discussion

A CH_2Cl_2 solution of the cluster dianion $[(Ph_3P)_2N]_2[Os_9(CO)_{24}]$ [6] reacts with the digold reagent Au_2Cl_2L (where L = bis-(diphenylphosphino)-methane (DPPM) or 1,2-bis-(diphenylphosphino)ethane (DPPE)) in the presence of the halide abstractor $TlPF_6$ to give, after purification, a brown neutral cluster compound as the only isolable product. On the basis of spectroscopic data the cluster has been formulated as $[Os_9(CO)_{23}(Au_2L)]$ ((**1a**) L = DPPM, (**1b**) L = DPPE), where not only has coordination of the digold fragment occurred, but a carbonyl ligand has been ejected from the cluster. In contrast, two brown products were isolated when the reaction was performed using the monogold electrophilic reagent $AuPR_3(NO)_3$ (where R = Ph, Cy). From the chromatographic properties and the spectroscopic data of these compounds, one has been identified as the neutral cluster $[Os_9(CO)_{24}\{Au(PR_3)\}_2]$ ((**2a**) R = Ph, (**2b**) R = Cy), whilst the other product has been formulated as the anionic cluster $[(Ph_3P)_2N][Os_9(CO)_{24}\{Au(PR_3)\}]$ ((**3a**) R = Ph, (**3b**) R = Cy). The $^{31}P\{^1H\}$ NMR spectra of the compounds (**1a**) and (**1b**) exhibit two resonances of equal intensity, indicating that the gold atoms are in non-equivalent environments and that these sites do not exchange to any significant degree on the NMR time scale at room temperature. In contrast, only one resonance was observed in the $^{31}P\{^1H\}$ NMR spectra of (**2a**) and (**2b**), implying that either the two gold atoms were coordinated in equivalent sites or they were rapidly exchanging. For the anionic compounds (**3a**) and (**3b**) two resonances are observed with a ratio of 2:1, the more intense peak being attributable to the cation $[(Ph_3P)_2N]^+$.

The molecular structure of $[Os_9(CO)_{23}(Au_2DPPE)]$ (**1b**) has been determined by a single crystal X-ray diffraction analysis (Fig. 1) and selected bond lengths

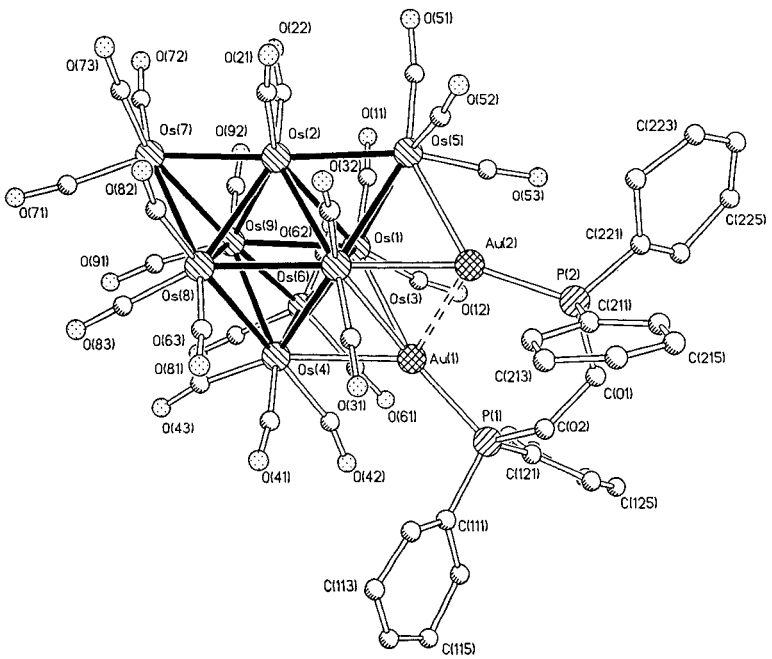

Fig. 1. Diagram depicting molecular structure of $[Os_9(CO)_{23}\{Au_2(DPPE)\}]$ (**1b**).

are presented in Table 1. The central metal geometry may be described as a tricapped octahedron of osmium atoms, with one of the gold atoms also capping an octahedral face and the remaining gold atom bridging between the octahedron and a capping osmium atom, adopting the asymmetric $\mu_3\,\mu_2$ bonding mode (Fig. 2). The osmium–osmium bond lengths vary quite dramatically within the cluster, ranging from 2.605(2) for Os(1)–Os(3) to 3.035(2) Å for Os(3)–Os(4) and having an average value of 2.82 Å. The general trend within this distribution of distances is that the osmium atoms with the highest metal–metal connectivity are associated with the shortest bond lengths, but there are several significant exceptions to this trend, notably in bonds to Os(4). The gold atoms form interactions with the osmium centres ranging from 2.719(2)–2.923(2) Å, making the shortest bonds to Os(1) and Os(3), which themselves have the highest metal–metal connectivity. The two gold atoms are at a distance of 2.837(2) Å from one another, hence there is the possibility of a significant bonding interaction between them. This variability of bond distances seems to be a feature of many high nuclearity metal clusters; this may be a consequence of the greater flexibility within the metal framework, due to less stringent directional constraints on metal–metal interactions as a result of increased electron delocalisation, or because there is a significant contribution of 'metal character' into the cluster bonding. The observed geometry for (**1b**) is remarkably similar to that reported [5] for the octaosmium cluster $[Os_8(CO)_{22}(Au_2DPPB)]$ (**4**), except that an additional face of the octahedron has been capped by an $Os(CO)_3$ unit. In addition, the tricapped octahedral osmium metal core of (**1b**) is the same geometry as that observed for the related cluster $[(Ph_3P)_2N][Os_9H(CO)_{24}]$ [6] (**5**), and although the structure of the precursor dianionic cluster $[(Ph_3P)_2N]_2[Os_9(CO)_{24}]$ (**6**) has not been determined experimentally, there is good evidence that it is also possesses a tricapped octahedral metal geometry. Whilst there appears to be no obvious correlation of the metal–metal distances between the three clusters, the average osmium–osmium bond lengths in (**4**) and (**5**) of 2.86 and 2.84 Å respectively, are not dissimilar to that of 2.82 Å observed for (**1b**). Indeed the average osmium–gold distance of 2.85 Å found in the cluster (**4**) is in accord with a value of 2.83 Å for (**1b**). It is noteworthy that the osmium–osmium bond lengths for (**1b**) show a greater variation than for those observed for both (**4**) and (**5**) and may possibly be due to the steric requirements of the digold moiety and the increased flexibility within the metal framework of (**1b**).

Table 1
Selected bond lengths (Å) for $[Os_9(CO)_{23}\{Au_2(DPPE)\}]$ (**1b**)

Au(1)–P(1)	2.318(10)	Os(2)–Os(9)	2.752(2)
Au(1)–Os(1)	2.819(2)	Os(2)–Os(5)	2.755(2)
Au(1)–Os(3)	2.826(2)	Os(2)–Os(3)	2.780(2)
Au(1)–Au(2)	2.837(2)	Os(2)–Os(8)	2.859(2)
Au(1)–Os(4)	2.923(2)	Os(3)–Os(8)	2.802(2)
Au(2)–P(2)	2.275(9)	Os(3)–Os(5)	2.879(2)
Au(2)–Os(3)	2.719(2)	Os(3)–Os(4)	3.035(2)
Au(2)–Os(5)	2.874(2)	Os(4)–Os(9)	2.778(2)
Os(1)–Os(3)	2.605(2)	Os(4)–Os(6)	2.945(2)
Os(1)–Os(9)	2.753(2)	Os(4)–Os(8)	2.970(2)
Os(1)–Os(5)	2.784(2)	Os(6)–Os(9)	2.685(2)
Os(1)–Os(6)	2.812(2)	Os(7)–Os(9)	2.762(2)
Os(1)–Os(2)	2.866(2)	Os(7)–Os(8)	2.936(2)
Os(1)–Os(4)	2.902(2)	Os(8)–Os(9)	2.839(2)
Os(2)–Os(7)	2.721(2)		

The solid-state molecular structure of $[Os_9(CO)_{24}\{Au(PCy_3)\}_2]$ (**2b**) has also been determined by X-ray crystallography (Fig. 3) and selected bond lengths are presented in Table 2. The observed geometry of the osmium core is best described as a bicapped octahedron of osmium atoms, where an edge of the octahedron is bridged by a further osmium atom Os(9) (Fig. 4). The two gold atoms may be thought to cap the

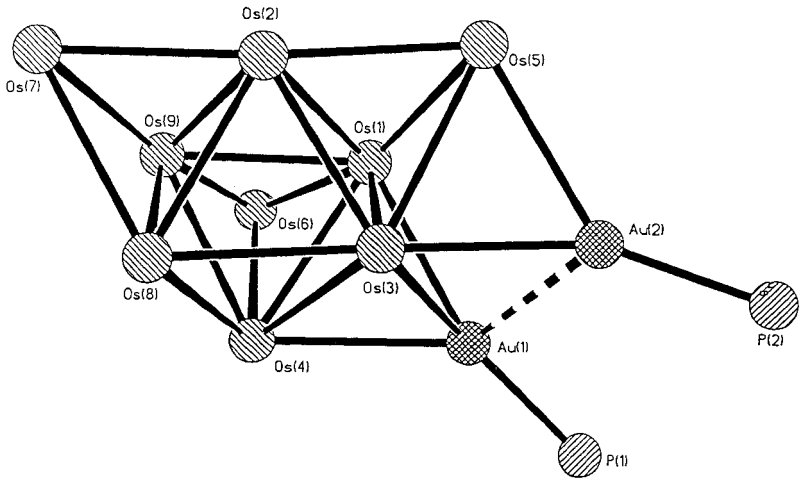

Fig. 2. Diagram depicting metal core geometry of $[Os_9(CO)_{23}\{Au_2(DPPE)\}]$ (**1b**).

opposite sides of the pseudo Os_4 'butterfly' described by the atoms Os(3), Os(5), Os(7) and Os(9), and with the gold atoms separated by a distance of 4.68 Å it is unlikely that there is any significant bonding interaction between them. The osmium–osmium bond lengths within the cluster range from 2.694(3) to 2.965(3) Å and have an average value of 2.85 Å. The observed cluster geometry is similar to that reported [7] for the related octaosmium digold cluster $[Os_8(CO)_{22}\{Au(PPh_3)\}_2]$ (**7**), where the osmium metal geometry was described as an octahedron with one edge bridged by two more osmium atoms. Although there are similarities in the gross overall metal framework between the clusters (**2b**) and (**7**), there are several distinctive differences between the two structures. These differences are most pronounced for the so-called 'wing-tip' atoms of the pseudo Os_4 'butterfly', which are separated by 3.373(3) Å in (**7**), whereas in (**2b**) they are significantly closer at 3.224(3) Å. In addition, for (**7**), these atoms are thought not to interact to any significant degree with the apical osmium atoms of the octahedron, being at a distance of 3.142(3) and 3.108(3) Å from them. Contrasting this for (**2b**), one apex of the octahedron is bound to a 'wing-tip' osmium atom (Os(2)–Os(3); 2.965(3) Å), whereas the other pair of atoms (Os(8), Os(9)) are separated by a distance of 3.391(3) Å and, as such, it is unlikely that any bonding interaction exists between them. From the overall molecular structure observed for (**2b**), it is apparent that a major reorganisation of the cluster's metal framework has occurred from that of the tricapped octahedral geometry of the precursor dianionic cluster $[(Ph_3P)_2N]_2[Os_9(CO)_{24}]$ [6].

Table 2
Selected bond lengths (Å) for $[Os_9(CO)_{24}\{Au(PCy_3)\}_2]$ (**2b**)

Os(1)–Os(2)	2.694(3)	Os(4)–Os(6)	2.861(2)
Os(1)–Os(4)	2.940(2)	Os(4)–Os(8)	2.874(5)
Os(1)–Os(6)	2.918(2)	Os(5)–Os(7)	2.870(2)
Os(2)–Os(3)	2.965(3)	Os(5)–Os(8)	2.926(4)
Os(2)–Os(4)	2.877(4)	Os(5)–Os(9)	2.779(2)
Os(2)–Os(5)	2.738(4)	Os(5)–Au(2)	2.784(2)
Os(2)–Os(6)	2.867(4)	Os(6)–Os(7)	2.849(2)
Os(2)–Os(7)	2.738(3)	Os(6)–Os(8)	2.859(4)
Os(3)–Os(5)	2.793(2)	Os(7)–Os(8)	2.916(4)
Os(3)–Os(7)	2.816(2)	Os(7)–Os(9)	2.777(2)
Os(3)–Au(1)	2.974(2)	Os(7)–Au(1)	2.807(2)
Os(3)–Au(2)	3.029(2)	Os(9)–Au(1)	2.907(2)
Os(4)–Os(5)	2.846(2)	Os(9)–Au(2)	2.978(2)

The observed molecular geometries of (**1b**) and (**2b**) are in agreement with the spectroscopic data, which indicated the coordination of the two gold atoms in non-equivalent environments for (**1a**) and (**1b**), whereas both gold atoms were thought to be bound in equivalent sites for (**2a**) and (**2b**). From these results it seems reasonable to assume that the geometries of the clusters, as determined in the solid state, are retained to a significant degree in solution.

There appears to be a clear similarity in the reactivity of the octa- and nona-osmium dianionic clusters $[(Ph_3P)_2N]_2[Os_8(CO)_{22}]$ (**8**) and $[(Ph_3P)_2N]_2[Os_9(CO)_{24}]$ (**6**) towards gold electrophilic reagents. For both compounds, reaction with mononuclear gold fragments results in the formation of a cluster in which a substantial metal core rearrangement has occurred,

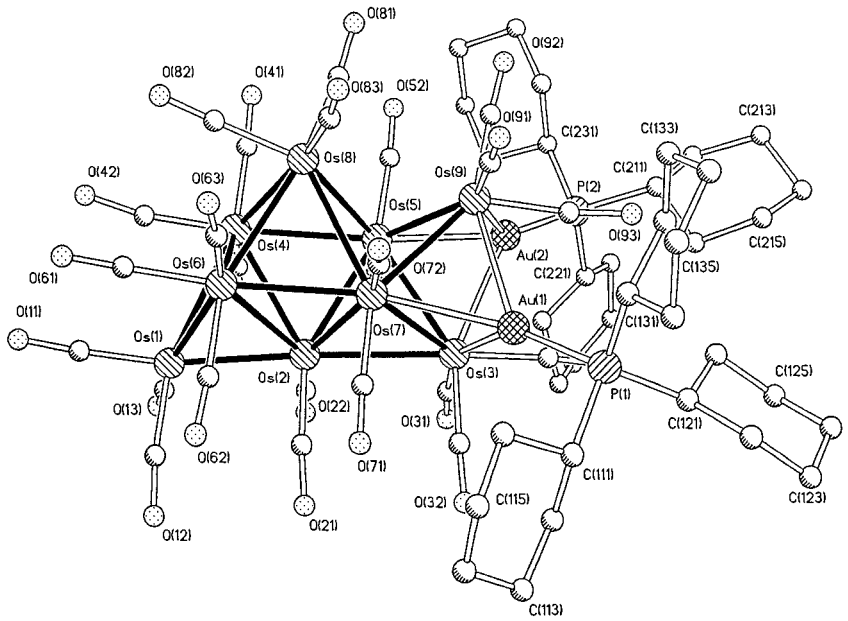

Fig. 3. Diagram depicting molecular structure of $[Os_9(CO)_{24}\{Au(PCy_3)\}_2]$ (**2b**).

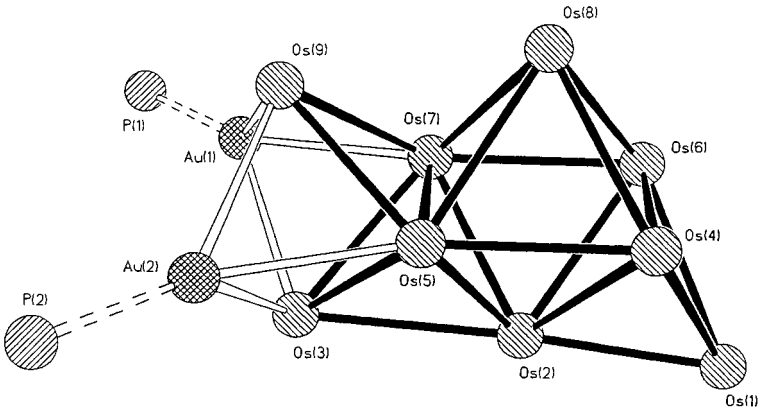

Fig. 4. Diagram depicting metal core geometry of $[Os_9(CO)_{24}\{Au(PCy_3)\}_2]$ (**2b**).

whereas reaction with a digold reagent (where the gold centres are connected with a bidentate phosphine) results in the formation of a product where the osmium metal framework remains identical to that of the starting material. The exact reasons why such a reactivity difference exists remain unclear; however, we have shown previously that when mononuclear gold fragments react with the octaosmium cluster (**8**) a kinetically favoured product is initially formed and that this rearranges to give (**7**), which may be thought of as the thermodynamically favoured product. No evidence of the formation of an intermediate product was observed for the analogous nona-osmium compound; however, it is feasible that rearrangement of the larger cluster is more facile and that reorganisation occurs rapidly at ambient temperatures. Another important factor to take into consideration, is that when (**6**) reacts with the digold reagent ''Au_2L^{2+}'' a carbonyl ligand is lost, whereas no removal of a carbonyl group was observed for the reaction with (**8**). This is probably due to the greater steric crowding that occurs between the ligands at the cluster surface as the number of metal atoms increases. However, the possibility that the reaction is proceeding via a different pathway for the larger cluster may not be entirely discounted. Another important difference in the reactivity between the octa- and nona-osmium clusters, is that a monoanionic product is formed in the reaction between (**6**) and the mononuclear gold electrophiles, whereas no analogous compound was isolated for (**8**). The formation of this anionic product may be rationalised in terms of the relative charge density on the cluster after coordination of the first gold fragment. Whilst both the mono-substituted octa- and nona-osmium compounds would carry a negative charge, this would be delocalised to a greater extent on the larger cluster, deactivating it to some extent towards further reaction with the electrophilic gold reagent. This apparent deactivation of the cluster is not observed when the reaction is performed using the digold fragments, with the second gold atom being held in close proximity to the cluster after the initial coordination. Although no evidence was obtained which could be used to unambiguously assign the structures of the mono-substituted clusters (**3a**) and (**3b**), it seems likely that these will have a tricapped octahedral geometry.

The formal electron count for compound (**1b**) is 120; however, if it is assumed that the cluster consists of a tricapped octahedron, then this has an electron count of 122 predicted from the 'polyhedral skeletal electron pair theory' for condensed polyhedra [8]. In comparison, (**2b**) has an observed electron count of 122 and, if the osmium framework is described as a bicapped octahedron with a further edge bridged, then the predicted electron count is 124 as determined by the condensed polyhedron method. However, if a bonding interaction is assumed between Os(3) and Os(9), or indeed between Os(8) and Os(9), then a predicted count of 122 electrons is obtained using this method.

3. Experimental

All reactions were performed under an atmosphere of purified dinitrogen by standard Schlenk and vacuum line techniques [9]. Subsequent work-up of products was carried out without precautions to exclude air. Solvents used were distilled from appropriate drying agents under dinitrogen. Routine separations of products were performed by thin layer chromatography using commercially prepared glass plates, precoated to 0.25 mm thickness with Merck Kieselgel 60 PF_{254}, or using laboratory-prepared glass plates coated to 1 mm thickness with Merck Kieselgel 60 PF_{254}.

IR spectra were recorded as dichloromethane solutions on a Perkin–Elmer 1710 Fourier transform spectrometer. ^1H and $^{31}P\{^1H\}$ NMR spectra were recorded on a Bruker AM-400 spectrometer and were referenced to external tetramethylsilane and trimethylphosphite respectively. Mass spectral data were obtained by the method of liquid secondary ion mass spectrometry

(LSIMS) on a Kratos MS-50 mass spectrometer, using *m*-nitrobenzylalcohol as a matrix. Elemental analyses were performed in this department by standard techniques. The compounds $[(Ph_3P)_2N]_2[Os_9(CO)_{24}]$, $Au(PR_3)NO_3$ (where R = Ph, Cy) and Au_2Cl_2L (where L = DPPM, DPPE) were prepared according to literature procedures [6,10,11].

*3.1. Preparation of $[Os_9(CO)_{23}(Au_2L)]$ (where L = DPPM (**1a**), DPPE (**1b**))*

To a solution of $[(Ph_3P)_2N]_2[Os_9(CO)_{24}]$ (50 mg, 15 μmol) in 25 ml of dichloromethane were added one equivalent of Au_2Cl_2L and an excess of the halide abstractor $TlPF_6$. The mixture was stirred at room temperature for 30 min, the solvent was removed and the residue purified by thin layer chromatography, eluting with a 60% CH_2Cl_2–*n*-hexane mixture to give the desired product in approximately 65% yield.

Spectroscopic data for (**1a**): IR ν_{CO} (CH_2Cl_2): 2092m, 2066m, 2050vs, 2026(sh), 2012m, 2001w(sh), 1936w(br) cm^{-1}. Positive ion LSIMS mass spectrum: *m/z* 3146 (observed), 3150 (calculated, based on ^{192}Os). $^{31}P\{^1H\}$ NMR (ppm, $CDCl_3$): δ −71.4 (d, 1P), −100.3 (d, 1P) $^2J(PP) = 72.9$ Hz. ^1H NMR (ppm, $CDCl_3$): δ 3.57–4.12 (m, 2H), 7.31–7.75 (m, 10H); (**1b**): IR ν_{CO} (CH_2Cl_2): 2091m, 2066m, 2049vs, 2026(sh), 2011m, 2001w(sh), 1995w(br) cm^{-1}. Positive ion LSIMS mass spectrum: *m/z* 3159 (observed), 3164 (calculated, based on ^{192}Os). $^{31}P\{^1H\}$ NMR (ppm, $CDCl_3$): δ −60.12 (s, 1P), −92.0 (s, 1P). ^1H NMR (ppm, $CDCl_3$): δ 2.48–3.35 (m, 4H), 7.41–7.72 (m, 10H).

*3.2. Preparation of $[Os_9(CO)_{24}(AuPR_3)_2]$ (where R = Ph (**2a**), Cy (**2b**)) and $[(Ph_3P)_2N][Os_9(CO)_{24}(AuPR_3)]$ (where R = Ph (**3a**), Cy (**3b**))*

To a solution of $[(Ph_3P)_2N]_2[Os_9(CO)_{24}]$ (50 mg, 15 μmol) in 25 ml of dichloromethane was added an excess of $Au(PR_3)NO_3$. The mixture was stirred at room temperature for 3 h, the solvent was removed and the residue purified by thin layer chromatography, eluting with a 60% CH_2Cl_2–*n*-hexane. In order of elution the neutral cluster compound ((**2a**) and (**2b**)) was obtained in 60% yield, whilst the mono-anionic product ((**3b**) and (**3b**)) was isolated in a yield of 25%.

Spectroscopic data for (**2a**): IR ν_{CO} (CH_2Cl_2): 2092m, 2064s, 2050(sh), 2042vs, 2013(sh), 2001m, 1954w(br) cm^{-1}. Positive ion LSIMS mass spectrum: *m/z* 3314 (observed), 3318 (calculated, based on ^{192}Os). $^{31}P\{^1H\}$ NMR (ppm, $CDCl_3$): δ −65.8 (s, 2P). ^1H NMR (ppm, $CDCl_3$): δ 7.32–7.67 (m, 30H); (**3a**): IR ν_{CO} (CH_2Cl_2): 2084w, 2049vs, 2039vs, 2019m, 1988s(br), 1972(sh), 1936w(sh) cm^{-1}. Negative ion LSIMS mass spectrum: *m/z* 2855 (observed), 2859 (calculated, based on ^{192}Os). $^{31}P\{^1H\}$ NMR (ppm, $CDCl_3$): δ −46.7 (s, 1P), −119.9 (s, 2P). ^1H NMR (ppm, $CDCl_3$): δ 7.38–7.71 (m, 45H); (**2b**): IR ν_{CO} (CH_2Cl_2): 2091m, 2061s, 2048(sh), 2040vs, 2009(sh), 1999m, 1969w(br) cm^{-1}. Positive ion LSIMS mass spectrum: *m/z* 3351 (observed), 3354 (calculated, based on ^{192}Os). $^{31}P\{^1H\}$ NMR (ppm, $CDCl_3$): δ −55.9 (s, 2P). ^1H NMR (ppm, $CDCl_3$): δ 1.46–1.88 (m, 66H); (**3b**): IR ν_{CO} (CH_2Cl_2): 2082w, 2049vs, 2039vs, 2018m, 1987m(br) cm^{-1}. Negative ion LSIMS mass spectrum: *m/z* 2878 (observed), 2877 (calculated, based on ^{192}Os). $^{31}P\{^1H\}$ NMR (ppm, $CDCl_3$): δ −70.0 (s, 1P), −119.9 (s, 2P). ^1H NMR (ppm, $CDCl_3$): δ 1.41–1.85 (m, 33H), 7.34–7.64 (m, 30H).

*3.3. Crystal structure determination for $[Os_9(CO)_{23}(Au_2DPPE)]$ (**1b**)*

$Os_9Au_2P_2O_{23}C_{49}H_{24}$, orthorhombic, space group $Pna2_1$, $a = 29.552(6)$, $b = 16.867(4)$, $c = 15.108(3)$ Å, $U = 7531(3)$ Å^3, $Z = 4$, $F(000) = 5496$, $\mu(Mo\,K\alpha) = 19.097\ mm^{-1}$, $D_c = 2.777\ g\,cm^{-3}$. A brown block-shaped crystal of approximate dimensions $0.15 \times 0.20 \times 0.20\ mm^3$ was mounted on a glass fibre, D_m not recorded, accurate lattice parameters determined from 25 reflections ($\theta = 15.10$–$16.89°$). Intensity data were measured on a Rigaku AFC7R diffractometer using monochromated Mo Kα radiation and ω scan mode to a maximum value for θ of 22.5°. Three standard reflections were monitored after every 100 reflections collected and showed an average decrease in standard intensity during the data collection time of −65%; a linear decay correction was applied to compensate for this apparent decay of X-ray intensity. A total of 7816 reflections were measured within the range $-21 \le h \le 31$, $-13 \le k \le 18$, $-16 \le l \le 16$ and averaged (Friedel opposites not merged) to yield 7150 unique reflections ($R_{int} = 0.0532$) of which 5464 were judged as significant by the criterion that $F_{obs} > 4\sigma(F_{obs})$. Corrections for Lorentz and polarisation effects were applied. Absorption corrections was applied using the method of Walker and Stuart [12], minimum and maximum corrections 0.719 and 1.220 respectively. Structure solution was by a combination of direct methods and Fourier techniques. Refinement of the 'Flack parameter' [13] to a value of −0.01(2) indicated that the correct absolute configuration had been assigned. Anisotropic thermal motion was assumed for the osmium, gold and phosphorus atoms. Hydrogen atoms were placed in calculated positions and refined using a riding model. Full matrix least squares refinement on F^2_{obs} for 7150 data and 405 parameters converged to $wR2 = 0.1169$ (all data), conventional $R = 0.0509$ (observed data), GOF (all data) = 1.031. The function minimised was $\sum w(F^2_{obs} - F^2_{calc})^2$, $w = 1/[\sigma^2(F^2_{obs}) + (0.0437P)^2 + 88.06P]$ where $P = (F^2_{obs} + 2F^2_{calc})/3$ and σ was obtained from counting statistics.

3.4. Crystal structure determination for $[Os_9(CO)_{24}\{Au(PCy_3)\}_2]$ (**2b**)

$Os_9Au_2P_2O_{24}C_{60}H_{66}$, triclinic, space group $P\bar{1}$, $a = 17.002(8)$, $b = 17.134(8)$, $c = 15.385(6)$ Å, $\alpha = 93.55(5)$, $\beta = 105.06(4)$, $\gamma = 116.19(4)°$, $U = 3802(3)$ Å^3, $Z = 2$, $F(000) = 2997$, $\mu(\text{Mo K}\alpha) = 18.939\,\text{mm}^{-1}$, $D_c = 2.932\,\text{g cm}^{-3}$. A brown block-shaped crystal of approximate dimensions $0.24 \times 0.28 \times 0.30\,\text{mm}^3$ was mounted on a glass fibre, D_m not recorded, accurate lattice parameters determined from 25 reflections ($\theta = 17.30$–$18.02°$). Intensity data were measured on a Rigaku AFC7R diffractometer using monochromated Mo Kα radiation and ω scan mode to a maximum value for θ of 22.5°. Three standard reflections were monitored after every 100 reflections collected and showed a decrease in standard intensity during the data collection time of −35%; a linear decay correction was applied to compensate for this apparent decay of X-ray intensity. A total of 12 021 reflections were measured within the range $0 \le h \le 18$, $-18 \le k \le 16$, $-16 \le l \le 16$ and averaged to yield 9975 unique reflections ($R_{int} = 0.0577$) of which 8952 were judged as significant by the criterion that $F_{obs} > 4\sigma(F_{obs})$. Corrections for Lorentz and polarisation effects were applied. Absorption corrections was applied using semi-empirical ψ scans, minimum and maximum transmission coefficients 0.3517 and 1.0000 respectively.

Table 3
Atomic coordinates and equivalent isotropic displacement parameters (Å^2) for (**1b**)

	x	y	z	U_{eq} [a]		x	y	z	U_{eq} [a]
Au(1)	0.22244(4)	0.14958(8)	0.1652	0.0548(4)	C(42)	0.1559(11)	0.088(2)	0.265(3)	0.055(10)
Au(2)	0.27151(5)	0.21578(9)	0.0217(2)	0.0657(5)	C(43)	0.0674(14)	0.084(2)	0.179(3)	0.089(14)
Os(1)	0.19522(4)	0.04031(7)	0.0345(2)	0.0447(4)	C(51)	0.2561(13)	0.030(2)	−0.198(3)	0.080(12)
Os(2)	0.15021(4)	0.08535(8)	−0.12586(14)	0.0473(4)	C(52)	0.2669(12)	0.183(2)	−0.175(3)	0.074(12)
Os(3)	0.18122(4)	0.19011(7)	0.0026(2)	0.0461(4)	C(53)	0.2962(13)	0.078(2)	−0.060(3)	0.078(12)
Os(4)	0.12654(4)	0.11019(7)	0.1474(2)	0.0492(4)	C(61)	0.1780(12)	−0.080(2)	0.260(3)	0.065(11)
Os(5)	0.24251(4)	0.10275(8)	−0.10888(14)	0.0512(4)	C(62)	0.1671(11)	−0.160(2)	0.107(3)	0.062(10)
Os(6)	0.14581(5)	−0.06112(8)	0.1462(2)	0.0558(4)	C(63)	0.090(2)	−0.106(3)	0.191(3)	0.10(2)
Os(7)	0.06105(4)	0.04968(9)	−0.1467(2)	0.0585(4)	C(71)	−0.0013(11)	0.046(2)	−0.123(2)	0.054(9)
Os(8)	0.08761(4)	0.17293(8)	−0.0198(2)	0.0532(4)	C(72)	0.0570(11)	−0.043(2)	−0.203(3)	0.066(10)
Os(9)	0.10474(4)	0.00926(7)	0.0085(2)	0.0479(4)	C(73)	0.0528(12)	0.103(2)	−0.257(3)	0.067(11)
P(1)	0.2661(3)	0.1973(5)	0.2811(7)	0.057(3)	C(81)	0.0862(14)	0.270(3)	0.031(3)	0.099(14)
P(2)	0.3369(3)	0.2707(5)	0.0722(7)	0.058(3)	C(82)	0.0687(13)	0.225(2)	−0.124(3)	0.085(13)
O(11)	0.2157(7)	−0.1018(13)	−0.080(2)	0.061(6)	C(83)	0.0287(13)	0.154(2)	0.024(3)	0.075(11)
O(12)	0.2645(8)	−0.0404(14)	0.155(2)	0.077(7)	C(91)	0.0449(12)	−0.019(2)	0.032(3)	0.072(11)
O(21)	0.1600(9)	0.186(2)	−0.293(2)	0.098(9)	C(92)	0.1116(11)	−0.091(2)	−0.041(3)	0.058(10)
O(22)	0.1584(7)	−0.0585(14)	−0.240(2)	0.064(7)	C(01)	0.3453(11)	0.251(2)	0.187(2)	0.064(10)
O(31)	0.1845(8)	0.346(2)	0.109(2)	0.076(7)	C(02)	0.3048(12)	0.273(2)	0.240(3)	0.071(11)
O(32)	0.1835(9)	0.305(2)	−0.152(2)	0.094(9)	C(111)	0.2284(12)	0.248(2)	0.360(3)	0.071(11)
O(41)	0.1081(9)	0.274(2)	0.221(2)	0.095(9)	C(112)	0.2035(12)	0.305(2)	0.340(3)	0.078(12)
O(42)	0.1627(9)	0.078(2)	0.336(2)	0.092(9)	C(113)	0.173(2)	0.349(3)	0.390(3)	0.099(14)
O(43)	0.0347(9)	0.061(2)	0.216(2)	0.089(8)	C(114)	0.177(2)	0.320(3)	0.480(4)	0.13(2)
O(51)	0.2592(11)	−0.013(2)	−0.262(2)	0.114(11)	C(115)	0.203(2)	0.269(3)	0.517(4)	0.13(2)
O(52)	0.2813(11)	0.231(2)	−0.227(2)	0.116(11)	C(116)	0.2322(13)	0.228(2)	0.452(3)	0.082(13)
O(53)	0.3322(10)	0.051(2)	−0.029(2)	0.103(9)	C(121)	0.2978(12)	0.127(2)	0.343(3)	0.068(11)
O(61)	0.1971(11)	−0.090(2)	0.322(2)	0.112(11)	C(122)	0.2850(13)	0.048(2)	0.347(3)	0.084(12)
O(62)	0.1750(9)	−0.222(2)	0.085(2)	0.098(9)	C(123)	0.303(2)	−0.007(3)	0.401(3)	0.11(2)
O(63)	0.0580(10)	−0.128(2)	0.218(2)	0.099(9)	C(124)	0.339(2)	0.013(4)	0.447(4)	0.14(2)
O(71)	−0.0402(10)	0.041(2)	−0.115(2)	0.103(9)	C(125)	0.357(3)	0.088(5)	0.432(6)	0.22(4)
O(72)	0.0586(10)	−0.104(2)	−0.243(2)	0.106(10)	C(126)	0.337(2)	0.147(3)	0.388(3)	0.10(2)
O(73)	0.0498(10)	0.135(2)	−0.324(2)	0.113(11)	C(211)	0.3397(11)	0.374(2)	0.061(3)	0.063(10)
O(81)	0.0842(10)	0.340(2)	0.051(2)	0.107(10)	C(212)	0.3001(12)	0.420(2)	0.054(2)	0.064(10)
O(82)	0.0673(9)	0.265(2)	−0.190(2)	0.093(9)	C(213)	0.3031(13)	0.505(2)	0.046(3)	0.083(12)
O(83)	−0.0073(9)	0.150(2)	0.049(2)	0.092(9)	C(214)	0.3451(13)	0.541(3)	0.041(3)	0.093(13)
O(91)	0.0085(9)	−0.037(2)	0.055(2)	0.085(8)	C(215)	0.3837(12)	0.497(2)	0.053(3)	0.069(11)
O(92)	0.1175(8)	−0.1522(14)	−0.071(2)	0.071(7)	C(216)	0.3817(11)	0.413(2)	0.062(2)	0.063(10)
C(11)	0.2109(10)	−0.041(2)	−0.039(2)	0.048(8)	C(221)	0.3877(9)	0.231(2)	0.025(2)	0.043(8)
C(12)	0.2366(10)	−0.011(2)	0.116(2)	0.049(9)	C(222)	0.389(2)	0.253(3)	−0.073(4)	0.13(2)
C(21)	0.1533(13)	0.147(2)	−0.235(3)	0.080(12)	C(223)	0.433(2)	0.222(3)	−0.108(4)	0.14(2)
C(22)	0.1600(11)	−0.001(2)	−0.191(3)	0.061(10)	C(224)	0.464(2)	0.176(3)	−0.075(4)	0.14(2)
C(31)	0.1840(11)	0.280(2)	0.071(3)	0.063(10)	C(225)	0.457(2)	0.159(3)	0.006(4)	0.11(2)
C(32)	0.1841(14)	0.261(3)	−0.097(3)	0.089(13)	C(226)	0.4165(14)	0.189(3)	0.062(3)	0.10(2)
C(41)	0.1181(13)	0.217(2)	0.194(3)	0.079(12)					

[a] U_{eq} is defined as one-third of the trace of the orthogonalised U_{ij} tensor.

Structure solution was by a combination of direct methods and Fourier techniques. During the refinement process it became apparent that there was approximately 20% disorder of Os(1), with its alternative position capping the face consisting of atoms Os(4), Os(6), Os(8). Alternative positions were also located and assigned to Os(2) and Os(8); however, due to the relatively small proportion of disorder, no alternative sites for the carbonyl ligands were located or assigned. In addition, the chlorine atoms of a molecule of CH_2Cl_2 with 20% occupancy were located and included in subsequent refinement. Anisotropic thermal motion was assumed for the osmium, gold and phosphorus atoms. Hydrogen atoms were placed in calculated positions and

Table 4
Atomic coordinates and equivalent isotropic displacement parameters (Å^2) for (**2b**)

	x	y	z	U_{eq} [a]		x	y	z	U_{eq} [a]
Os(3)	−0.21398(6)	−0.35554(5)	−0.80547(6)	0.0463(2)	C(42)	0.233(2)	−0.173(2)	−0.797(2)	0.067(6)
Os(4)	0.12747(6)	−0.21252(6)	−0.76334(6)	0.0496(2)	C(43)	0.124(2)	−0.322(2)	−0.749(2)	0.061(6)
Os(5)	−0.02735(5)	−0.25738(5)	−0.70018(5)	0.0412(2)	C(51)	−0.028(2)	−0.3627(14)	−0.679(2)	0.053(5)
Os(6)	0.04829(6)	−0.14620(6)	−0.90839(6)	0.0474(2)	C(52)	0.043(2)	−0.2168(14)	−0.577(2)	0.050(5)
Os(7)	−0.10683(5)	−0.19070(5)	−0.84550(5)	0.0394(2)	C(61)	0.157(2)	−0.102(2)	−0.942(2)	0.064(6)
Os(9)	−0.11992(6)	−0.16426(5)	−0.67097(5)	0.0406(2)	C(62)	−0.027(2)	−0.188(2)	−1.032(2)	0.058(6)
Au(1)	−0.28002(5)	−0.22179(5)	−0.83405(6)	0.0463(2)	C(63)	0.062(2)	−0.031(2)	−0.912(2)	0.060(6)
Au(2)	−0.14611(6)	−0.32780(5)	−0.59783(6)	0.0484(2)	C(71)	−0.1820(14)	−0.2317(13)	−0.9672(14)	0.046(5)
P(1)	−0.4110(4)	−0.2054(4)	−0.8793(4)	0.0500(13)	C(72)	−0.114(2)	−0.087(2)	−0.867(2)	0.054(5)
P(2)	−0.1816(4)	−0.3939(4)	−0.4773(4)	0.0531(14)	C(81)	0.126(2)	−0.036(2)	−0.594(2)	0.063(6)
Os(1)	0.07254(8)	−0.29992(7)	−0.95560(8)	0.0511(3)	C(82)	0.194(2)	−0.007(2)	−0.734(2)	0.056(11)
Os(2)	−0.0606(2)	−0.3207(2)	−0.8809(2)	0.0382(5)	C(83)	0.0589(14)	0.0221(14)	−0.7218(14)	0.049(5)
Os(8)	0.0806(2)	−0.0758(2)	−0.7217(3)	0.0422(6)	C(91)	−0.1295(13)	−0.0572(13)	−0.6891(13)	0.043(5)
Os(1B)	0.2201(4)	−0.0158(4)	−0.7382(5)	0.057(2)	C(92)	−0.0539(14)	−0.1207(13)	−0.5465(14)	0.045(5)
Os(2B)	0.0532(9)	−0.0929(10)	−0.7125(12)	0.045(3)	C(93)	−0.224(2)	−0.203(2)	−0.636(2)	0.065(6)
Os(8B)	−0.0335(7)	−0.3191(10)	−0.8881(10)	0.038(2)	C(111)	−0.454(2)	−0.222(2)	−1.008(2)	0.066(6)
Cl(1)	−0.549(3)	−0.116(3)	−0.599(3)	0.086(10)	C(121)	−0.510(2)	−0.287(2)	−0.850(2)	0.083(8)
Cl(2)	−0.390(4)	−0.124(4)	−0.501(4)	0.13(2)	C(131)	−0.387(2)	−0.092(2)	−0.840(2)	0.063(6)
O(11)	0.241(2)	−0.225(2)	−1.015(2)	0.144(10)	C(211)	−0.255(2)	−0.361(2)	−0.432(2)	0.079(7)
O(12)	−0.054(2)	−0.391(2)	−1.150(2)	0.108(7)	C(221)	−0.240(2)	−0.516(2)	−0.506(2)	0.082(8)
O(13)	0.096(2)	−0.464(2)	−0.935(2)	0.107(7)	C(231)	−0.076(2)	−0.3591(14)	−0.380(2)	0.055(5)
O(21)	−0.1994(13)	−0.4074(12)	−1.0694(13)	0.081(5)	C(112)	−0.480(3)	−0.313(2)	−1.056(3)	0.121(12)
O(22)	−0.0737(11)	−0.5013(11)	−0.8667(11)	0.068(4)	C(113)	−0.509(3)	−0.325(3)	−1.158(3)	0.15(2)
O(31)	−0.2335(14)	−0.5386(14)	−0.8017(14)	0.094(6)	C(114)	−0.449(3)	−0.251(3)	−1.188(3)	0.16(2)
O(32)	−0.3581(13)	−0.4380(12)	−0.9899(13)	0.084(5)	C(115)	−0.420(3)	−0.159(3)	−1.147(3)	0.125(13)
O(33)	−0.3761(14)	−0.4176(13)	−0.7314(14)	0.090(6)	C(116)	−0.382(2)	−0.155(2)	−1.042(2)	0.096(9)
O(41)	0.2514(13)	−0.1356(12)	−0.5662(13)	0.081(5)	C(122)	−0.601(2)	−0.283(2)	−0.889(3)	0.106(10)
O(42)	0.309(2)	−0.135(2)	−0.808(2)	0.111(7)	C(123)	−0.685(3)	−0.366(3)	−0.876(3)	0.16(2)
O(43)	0.1337(12)	−0.3838(12)	−0.7372(12)	0.077(5)	C(124)	−0.666(3)	−0.379(3)	−0.787(3)	0.112(11)
O(51)	−0.0224(12)	−0.4260(11)	−0.6615(12)	0.075(5)	C(125)	−0.583(2)	−0.384(2)	−0.751(3)	0.112(11)
O(52)	0.0922(12)	−0.1923(11)	−0.4990(12)	0.070(4)	C(126)	−0.496(3)	−0.298(3)	−0.761(3)	0.125(13)
O(61)	0.220(2)	−0.0684(14)	−0.966(2)	0.100(6)	C(132)	−0.361(2)	−0.065(2)	−0.735(2)	0.067(6)
O(62)	−0.0677(12)	−0.2119(11)	−1.1085(12)	0.069(4)	C(133)	−0.322(2)	0.034(2)	−0.705(2)	0.092(9)
O(63)	0.0752(11)	0.0405(11)	−0.9161(11)	0.069(4)	C(134)	−0.383(3)	0.068(3)	−0.753(3)	0.123(12)
O(71)	−0.2308(12)	−0.2538(11)	−1.0412(12)	0.069(4)	C(135)	−0.410(3)	0.043(2)	−0.850(2)	0.115(11)
O(72)	−0.1196(11)	−0.0264(10)	−0.8890(11)	0.065(4)	C(136)	−0.454(2)	−0.059(2)	−0.886(2)	0.093(9)
O(81)	0.1619(12)	−0.0009(11)	−0.5169(12)	0.073(5)	C(212)	−0.256(2)	−0.383(2)	−0.337(2)	0.101(10)
O(82)	0.266(2)	0.034(2)	−0.739(2)	0.110(8)	C(213)	−0.318(3)	−0.347(3)	−0.307(3)	0.16(2)
O(83)	0.0539(11)	0.0862(10)	−0.7260(11)	0.062(4)	C(214)	−0.417(3)	−0.386(3)	−0.371(3)	0.137(14)
O(91)	−0.1324(10)	0.0043(10)	−0.6952(10)	0.058(4)	C(215)	−0.406(3)	−0.357(3)	−0.461(3)	0.131(13)
O(92)	−0.0175(11)	−0.0891(10)	−0.4705(11)	0.063(4)	C(216)	−0.351(2)	−0.394(2)	−0.498(2)	0.080(8)
O(93)	−0.2877(13)	−0.2214(12)	−0.6047(13)	0.083(5)	C(222)	−0.244(3)	−0.567(2)	−0.432(2)	0.110(11)
C(11)	0.171(2)	−0.253(2)	−0.995(2)	0.092(9)	C(223)	−0.290(3)	−0.665(3)	−0.470(3)	0.15(2)
C(12)	0.001(3)	−0.353(3)	−1.076(3)	0.124(12)	C(224)	−0.290(3)	−0.700(3)	−0.549(3)	0.138(14)
C(13)	0.082(2)	−0.398(2)	−0.944(2)	0.089(9)	C(225)	−0.303(3)	−0.655(2)	−0.623(3)	0.113(11)
C(21)	−0.141(2)	−0.3735(14)	−0.996(2)	0.054(5)	C(226)	−0.232(3)	−0.553(3)	−0.579(3)	0.16(2)
C(22)	−0.069(2)	−0.433(2)	−0.872(2)	0.054(5)	C(232)	−0.013(2)	−0.392(2)	−0.404(2)	0.064(6)
C(31)	−0.221(2)	−0.466(2)	−0.800(2)	0.079(8)	C(233)	0.076(2)	−0.361(2)	−0.322(2)	0.099(10)
C(32)	−0.301(2)	−0.400(2)	−0.922(2)	0.060(6)	C(234)	0.123(2)	−0.263(2)	−0.289(2)	0.104(10)
C(33)	−0.312(2)	−0.391(2)	−0.756(2)	0.064(6)	C(235)	0.066(2)	−0.229(2)	−0.262(2)	0.079(7)
C(41)	0.202(2)	−0.164(2)	−0.643(2)	0.070(7)	C(236)	−0.025(2)	−0.261(2)	−0.343(2)	0.070(7)

[a] U_{eq} is defined as one-third of the trace of the orthogonalised U_{ij} tensor.

refined using a riding model, with the thermal parameters being held constant at 0.08 Å^2. Full matrix least squares refinement on F^2_{obs} for 9974 data and 489 parameters converged to $wR2 = 0.1402$ (all data), conventional $R = 0.0547$ (observed data), GOF (all data) = 1.129. The function minimised was $\sum w(F^2_{obs} - F^2_{calc})^2$, $w = 1/[\sigma^2(F_{obs^2}) + (0.0438P)^2 + 137.17P]$ where $P = (F^2_{obs} + 2F^2_{calc})/3$ and σ was obtained from counting statistics.

For both crystal structures all calculations were performed using the TEXSAN, SHELXS-86 and SHELXL-93 program packages [14–16]. Atomic coordinates and equivalent isotropic displacement parameters for **1b** and **2b** are listed in Tables 3 and 4 respectively. Additional information, comprising hydrogen atom coordinates, anisotropic thermal parameters and full listings of bond lengths and angles, has been deposited at the Cambridge Crystallographic Data Centre.

4. Conclusion

The results of the above study show that the cluster dianion $[(Ph_3P)_2N]_2[Os_9(CO)_{24}]$ reacts with the electrophilic monogold reagents ''$AuPR_3^+$'' to give both mono- and di-substituted products, where it has been found that the latter product has undergone a major rearrangement of the metal core geometry. In contrast reaction with the digold reagent ''Au_2L^{2+}'' results in the formation of a cluster where the osmium framework retains its original geometry, albeit with the loss of a carbonyl ligand. The isolation and characterisation of these products clearly demonstrate the flexibility that appears to be an inherent property of high nuclearity osmium carbonyl cluster compounds, which most likely arises from a subtle balance between the electronic properties of the metal core and the steric requirements of the ligand periphery.

Acknowledgements

We gratefully acknowledge the E.P.S.R.C. (S.L.I.), the Cambridge Commonwealth Trust and the UK Committee of Vice Chancellors and Principals (Z.A.) for financial support, Johnson Matthey for the loan of osmium salts, and the E.P.S.R.C. and The Cambridge Crystallographic Data Centre for assistance with the purchase of the X-ray equipment.

References

[1] (a) E. Charalambous, L.H. Gade, B.F.G. Johnson, T. Kotch, A.J. Lees, J. Lewis, M. McPartlin, Angew. Chem. Int. Ed. Engl. 29 (1990) 1137. (b) L.H. Gade, B.F.G. Johnson, J. Lewis, M. McPartlin, T. Kotch, A.J. Lees, J. Am. Chem. Soc. 113 (1991) 8698.
[2] (a) L.H. Gade, B.F.G. Johnson, J. Lewis, M. McPartlin, H.R. Powell, J. Chem. Soc. Chem. Commun. (1990) 110. (b) R. Della Pergola, F. Demartin, L. Garlaschelli, M. Manassero, S. Martinengo, N. Masciocchi, M. Sansoni, Organometallics 10 (1991) 2239. (c) A.J. Whoolery, L.F. Dahl, J. Am. Chem. Soc. 113 (1991) 6683. (d) A. Fumagalli, S. Martinengo, V.G. Albano, D. Braga, F. Grepioni, J. Chem. Soc. Dalton Trans. (1993) 2047. (e) V. Dearing, S.R. Drake, B.F.G. Johnson, J. Lewis, M. McPartlin, H.R. Powell, J. Chem. Soc. Chem. Commun. (1988) 1331.
[3] (a) L.H. Gade, B.F.G. Johnson, J. Lewis, M. McPartlin, H.R. Powell, J. Chem. Soc. Chem. Commun. (1992) 921. (b) L.H. Gade, Angew. Chem. Int. Ed. Engl. 32 (1993) 24. (c) J.W. Lauher, K. Wald, J. Am. Chem. Soc. 103 (1981) 7648. (d) L.W. Bateman, M. Green, J.A.K. Howard, K.A. Mead, R.M. Mills, I.D. Salter, F.G.A. Stone, P. Woodward, J. Chem. Soc. Chem. Commun. (1982) 773.
[4] (a) S.L. Ingham, J. Lewis, P.R. Raithby, J. Chem. Soc. Chem. Commun. (1993) 166. (b) Z. Akhter, S.L. Ingham, J. Lewis, P.R. Raithby, Angew. Chem. Int. Ed. Engl. 35 (1996) 992. (c) A.J. Amoroso, L.H. Gade, B.F.G. Johnson, J. Lewis, P.R. Raithby, W.-T. Wong, Angew. Chem. Int. Ed. Engl. 30 (1991) 107.
[5] Z. Akhter, S.L. Ingham, J. Lewis, P.R. Raithby, J. Organomet. Chem. 474 (1994) 165.
[6] A.J. Amoroso, B.F.G. Johnson, J. Lewis, P.R. Raithby, W.-T. Wong, J. Chem. Soc. Chem. Commun. (1991) 814.
[7] B.F.G. Johnson, J. Lewis, W.J.H. Nelson, P.R. Raithby, M.D. Vargas, J. Chem. Soc. Chem. Commun. (1983) 608.
[8] D.M.P. Mingos, J. Cherm. Soc. Chem. Commun. (1983) 706.
[9] D.F. Shriver, Manipulation of Air-Sensitive Compounds, McGraw-Hill, New York, 1969.
[10] A.M. Mueting, B.D. Alexander, P.D. Bole, A.L. Casalnuovo, L.N. Itp, B.J. Johnson, L.H. Pignolet, Inorg. Synth. 29 (1992) 280.
[11] S.J. Berners-Price, M.A. Mazid, P.J. Sadler, J. Chem. Soc. Dalton Trans. (1984) 969.
[12] N. Walker, D. Stuart, Acta Crystallogr. Sect. A: 39 (1983) 158.
[13] H.D. Flack, Acta Crystallogr. Sect. A: 39 (1983) 876.
[14] TEXSAN: Single Crystal Structure Analysis Software, Version 1.6, 1993, Molecular Structure Corporation, The Woodlands, TX 77381, USA.
[15] G.M. Sheldrick, Acta Crystallogr. Sect. A: 46 (1993) 467.
[16] G.M. Sheldrick, SHELXL-93, Program for Structure Refinement, University of Göttingen, 1993.